Original Article

e-ISSN: 2581-0545 - https://journal.itera.ac.id/index.php/jsat/

Hydrodynamic numerical investigation and sedimentation, a study cases in Lontar steam-electric power plant

Received 13th June 2023
Accepted 11th September 2023
Published 11th December 2023

Open Access

DOI: 10.35472/jsat.v7i2.1451

Suciana *[a], Alamsyah Kurniawan [b]

[a] *Ocean Engineering Study Program, Faculty of Infrastructure and Regional Technology, Institut Teknologi Sumatera, Lampung Selatan*

[b] *Ocean Engineering, Institut Teknologi Bandung, Bandung*

**Corresponding author: suciana@kl.itera.ac.id*

Abstract: The intake pump of the Lontar steam-electric power plant cannot operate optimally due to a drawdown in the forebay. The capacity of the conveying channel decreases, possibly caused by sedimentation at the intake mouth. So, an initial investigation is required using hydro-oceanographic and sedimentation numerical modeling in that area. Numerical modeling is conducted to simulate flow phenomena to obtain a model and measurement data for qualitative assessment. Hence, the flow condition in the study area is a mix of ocean current and circulating water pump discharge. Hydrodynamic modeling has been successfully conducted to assess their interaction in this zone properly by using open-source software called Delft3D Hydro-morphodynamic. This research uses primary data or field measurement data like bathymetry, sediment, and discharge data for input. Model calibration used tidal and current data. Based on the results of the numerical modeling, it is evident that sediment deposition occurs at the intake mouth area due to the suction of the circulating water pump unit, resulting in sediment being carried and deposited during high water levels and a slowing down of flow rate. Sedimentation issues can addressed through dredging, and for the long-term recommendation to install a breakwater to extend the dredging service life at the intake mouth.

Keywords: *Intake, steam-electric power plant, sedimentation, hydrodynamic, breakwater.*

Introduction

The Lontar steam-electric power plant, with a capacity of 3x315 MW, is located in Lontar Village, Tangerang Regency, Banten Province. The Lontar steam-electric power plant is one of the main power generation units in the western part of Java. During its operation, it was found that the intake pump could not function optimally due to a drawdown in the forebay. This has resulted in the overall suboptimal operation of the steam-electric power plant. The initial presumption for the decrease in the capacity of this conduct is the presence of sedimentation at the intake mouth leading to the Java Sea, causing obstruction in the discharge capacity at that point and resulting in a drawdown that extends to the forebay and pump pit. The aim of this study is to define the current velocity and patterns in the waters of the Lontar steam-electric power plant area, hydrodynamic modeling is required. Additionally, to determine the volume of dredging needed and minimize the possibility of future and unforeseen sedimentation events, sedimentation modeling is necessary.

This study investigates focuses on the water area at the mouth of the intake channel of the cooling water pump, located along the Java Sea coastline, as well as the land area, including the intake channel and circulating water pump forebay, as shown in **Figure 1**.

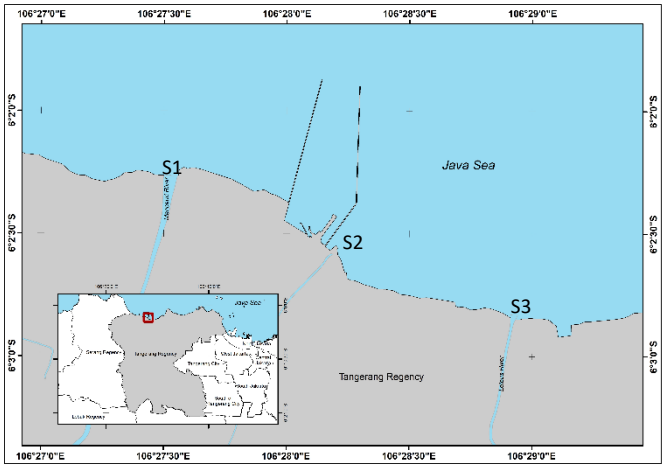

Figure 1. The study area

Previous studies have correlated, studied the characteristics of suspended sediment during spring and neep tides in summer, and found that intense sediment

suspension caused by the high water velocity was a significant cause of downstream channel siltation [6]. Also observed was an enhanced sediment resuspension effect in the downstream channel after the installation of a sluice gate. These studies have shown that when the sluice gate opens the scouring effect of the ebb current increases and this substantially reduces the amount of siltation [7]. Numerous studies have been conducted on various approaches to the numerical method [1], [10], [12], [15].

Materials and method

In this study, Delft3D is used for modeling purposes. Delft3D-FLOW is a hydrodynamic and transport model that solves the Navier-Stokes equation for an incompressible fluid under shallow water and Boussinesq assumptions [8]. The use of Delft3D provides convenience through its open-source program license. This means that the legality of using this modeling system can be accounted for [3]. The scheme of the process modeling in this study is illustrated in **Figure 2**.

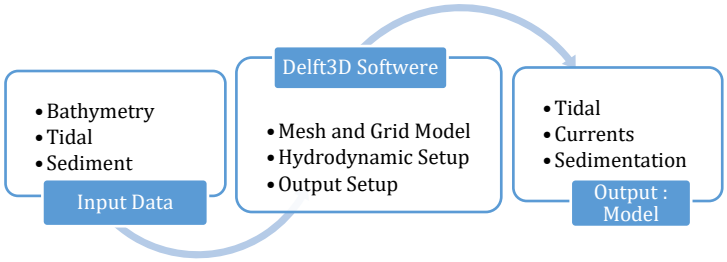

Figure 2. The schema of the process modeling

Field measurement

Field measurements including water level and bathymetry, were carried out along the Lontar steam electric power plant to calibrate the Delft3D model.

The primary data used as input for the model consists of bathymetric data. The first stage involved the use of a multibeam echosounder to map the harbor basin area, while the second stage utilized a single-beam echosounder to map the shallow areas, intake mouth, and canal up to the forebay of the cooling water pump and the outside area using secondary data bathymetric from national bathymetry (tanahair.indonesia.go.id). Bed levels were continuously updated based on a sediment transport field, which was defined by the derived flow field [5].

The next data is tide. Tide data was collected through direct field measurements over a period of 30 days with a tide gauge. The important tide water level elevation is shown in **Table 1**.

Table 1. Important Tide Water Level Elevations

	Local (0 palm)	Geodetik (Ellipsoid)	MSL (as built drawing 2011)
HWL	**2.353**	18.370	0.504
MSL	**1.849**	17.866	0.004
LWL	**1.312**	17.329	-0.537

In summary, based on the table above, it can be concluded that the predicted tidal range for the next 20 years is 1.041 meters, with the lowest ebb value from the Mean Sea Level (MSL) prediction being 0.537 meters and the highest tide reaching 0.504 meters. The values of these important elevations were projected into the geodetic height system and mean sea level based on the as-built drawing data. The tidal type in the study location is diurnal.

Sediment and water samples were obtained using a sediment grabber and water sampler. The sampling locations were selected at the three nearest river estuaries to the study site named S.1, S.2, and S3 in Figure 1.

Numerical Simulation

Modeling was conducted for the large area and small area. The purpose of creating the large area model (**Figure 3**) is to observe the offshore currents as the dumping area. Meanwhile, the purpose of creating the small area model was to examine the magnitude and patterns of currents, particularly within the breakwater area, and to observe sedimentation occurrences.

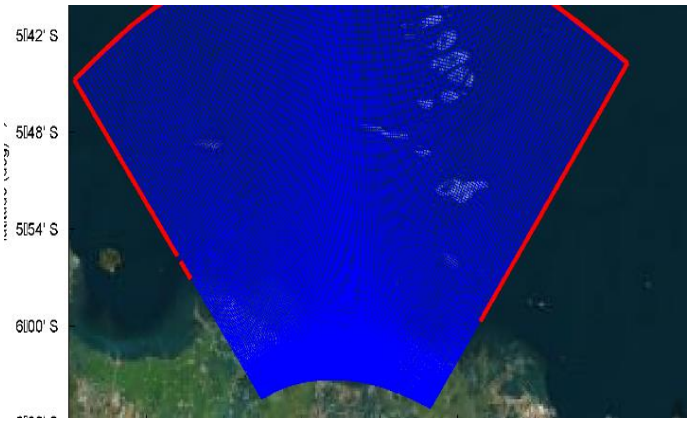

Figure 3. Computational domain (grid) of the large area

The numerical grid for the large area covers not only the area of interest but including the outer area until the deep water. The large mesh has a total of 36000 grids, with 200 grids in the M direction and 180 grids in the N direction. The grid size 600 m x 600 m at the boundary, and 100 m x 100 m in the focussed studied area.

The computational domain of the small area consists of 9020 grids, with 110 grids in the M direction and 82 grids in the N direction. The grid size ranges from 100 m x 100 m at the boundary and 10 m x 10 m in the studied area, as shown in **Figure 4.**

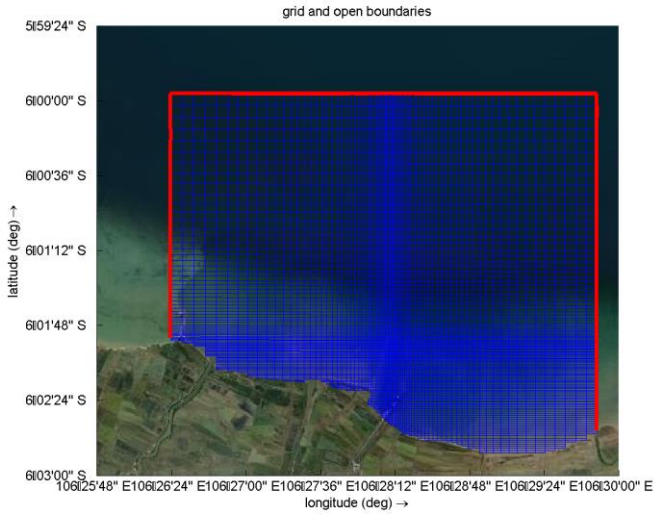

Figure 4. Computational domain (grid) of the small area

The modeling system for the horizontal direction uses a finite difference grid system in two coordinate systems, namely cartesian coordinates and spherical coordinates. As for the vertical direction, there is the sigma coordinate for atmospheric models and the z-layer for cartesian coordinates. For the open boundary (red line in **Figure 3** and **Figure 4**) all the relevant hydrodynamic and morphodynamic forcing factors are considered in the simulation. The tide is introduced by considering the values of the seven major tidal constituents provided by TPXO data [4]. In this study, tidal constituents at the open boundary can be seen in **Table 2.**

Table 2. Tidal constituents at the open boundary of the numerical grid

Constituent	Amplitude (cm)	Phase (°)
M2	0,35	189,88
S2	6,69	88,43
N2	1,69	200,09
K2	1,50	76,74
K1	24,01	49,82
O1	13,72	80,41
P1	6,27	71,31

The land boundary model was obtained from the satellite image, National Bathymetry, and National DEM dataset from the Indonesia Geospatial Information Agency (BIG,2000). The bathymetric data of the model (**Figure 5a**) are obtained from relevant nautical charts as national bathymetry maps, and from the field measurement in the area of interest which are digitized and interpolated onto the computational grid and then exported as depth model data.

From the bathymetry survey result the area interest, means the area channel is relatively shallow, the depth around is less than 7m. (**Figure 5b**)

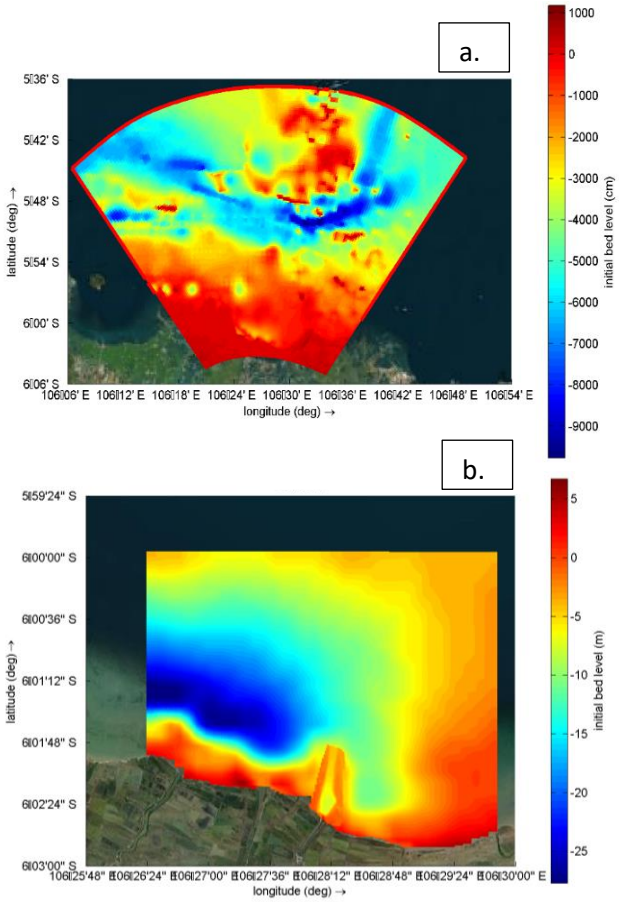

Figure 5. Bathymetry of the large area (a) and small area (b)

The bed roughness parameter is adjusted during the calibration process [1]. Since the bed condition in the study area is dominantly silty clay, the model uses a higher manning number (lower resistance) as suggested by [13]. The final model uses a higher manning constant value of 60, and the spatial distribution of the mean grain size diameter, D_{50} is input to the model using measured data. See **Table 3.**

Published by: Lembaga Penelitian dan Pengabdian Masyarakat (LPPM)
Institut Teknologi Sumatera, Lampung Selatan, Indonesia

Table 3. Principle parameters used in the numerical model sediment

Parameter	Sed.1	Sed.2	Sed.3
Specific density (Kg/m^3)	2650	2650	2650
Dry bed density (Kg/m^3)	1600	1600	1600
Median sediment diameter (D_{50})	0,009	0,014	0,034

Results and Discussion

The model was run for one month to validate the output model, the tidal model with tidal field data (time-series comparison). The validation results are presented in **Figure 6.** The figure shows that the phase and amplitude between the model and field data are consistent. The error value as the Pearson coefficient (R), is 0.87. Based on this validation, it can be concluded that the model reliably to simulates current patterns and water surface fluctuations.

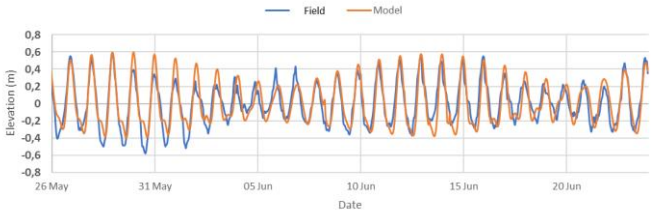

Figure 6. Time-series of tidal levels: model vs field data

The current velocity and the patterns of a large area can be seen in **Figure 7.** The red crossline means dumping area. The time series values of current at the dumping area location are shown in **Figure 8**. Statistically, It can be observed that the highest current value from the model reaches 0.9 m/s.

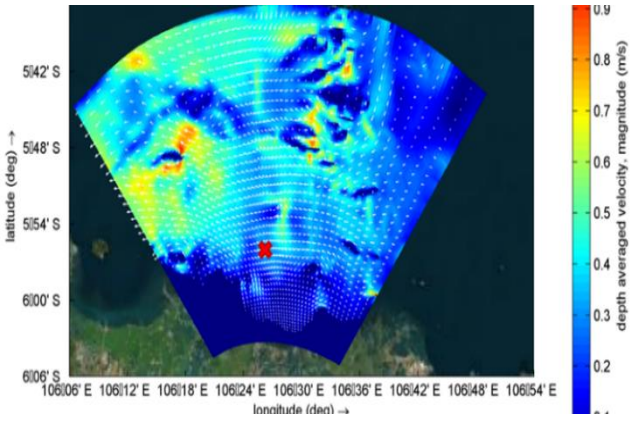

Figure 7. Current patterns in the large area

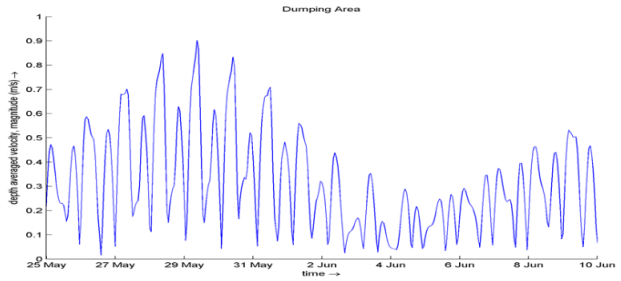

Figure 8. Time series of currents in the dumping area

The current velocity and the patterns of a small region can be seen in **Figure 9.** The current movement patterns within the vector in the channel area can be seen in **Figure 10,** The magnitude of the current model for the channel area is approximately 0.05-0.1 m/s. The result from the model simulations shows that the current velocity at low tide is higher than at high tide as the tidal current goes in one direction.

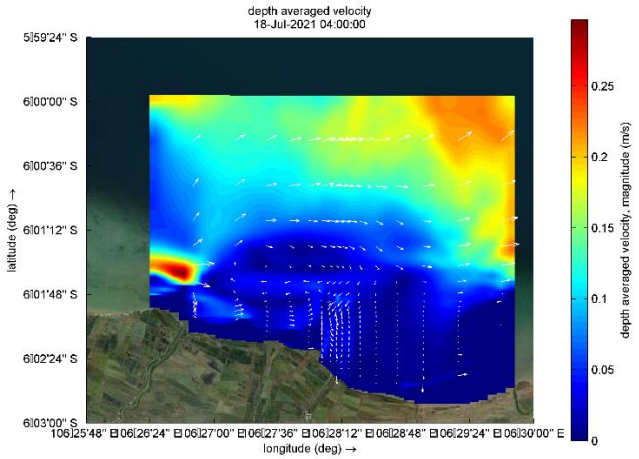

Figure 9. Values and patterns of current in a small area.

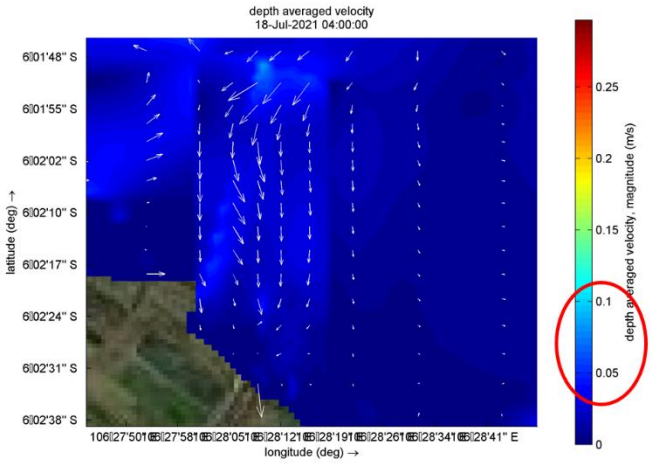

Figure 10. Values and patterns of current in the channel area.

According to [9] the velocity of water currents can be grouped into very fast (>1m/s), fast (0.5-1 m/s), medium (0.25 - 0.5m/s), slow (0.1 – 0.25 m/s) and very slow (<0.01 m/s). In conclusion, the study location's average current speed category is fast.

The validation of tidal has been a good result, so the sedimentation model could simulated for one year (2021-2022) to observe the sediment changes occur in the channel area, it is necessary to conduct a review by creating a longitudinal profile of 1200 meters towards the sea, which is drawn perpendicular as shown in **Figure 11.**

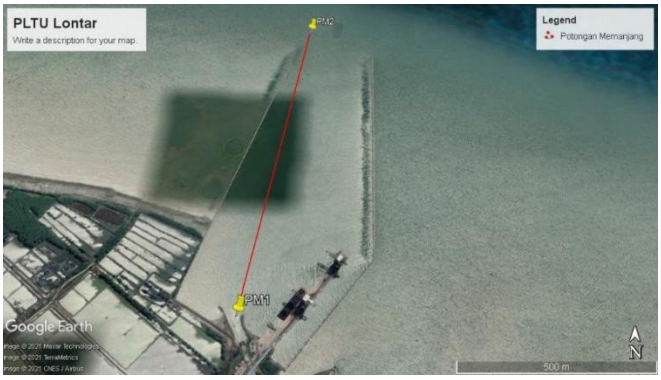

Figure 11. Longitudinal profile of 1200 m towards the sea.

From the model results, the graph of sedimentation values or sediment addition per quarter can be observed for the longitudinal section of the canal area in the existing condition. The sediment addition values per quarter in the existing condition can be seen in **Figure 12**.

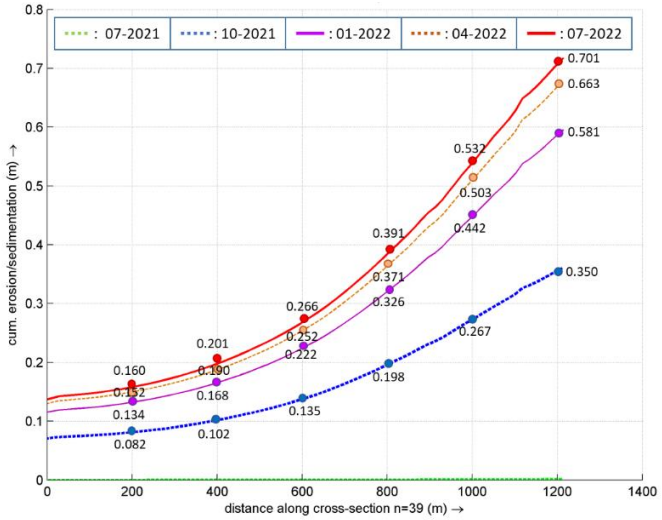

Figure 12. Graph of sediment addition values per quarterly in the existing condition.

The sediment addition leads to changes in the seabed. As we move towards the mouth of the breakwater, the sedimentation value increases. The changes in depth can be seen in **Figure 13.**

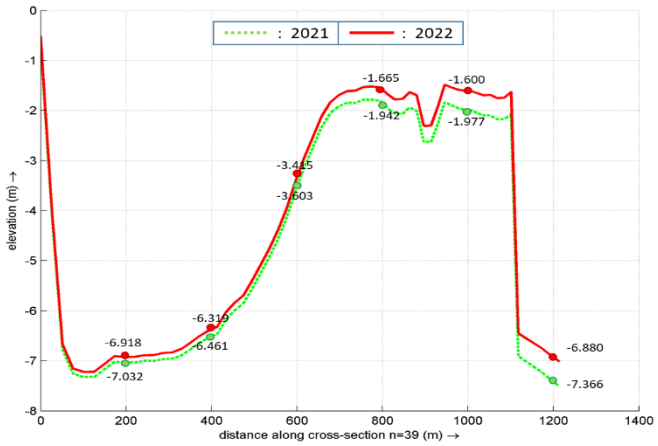

Figure 13. Graph of changes seabed in the existing condition.

Considering the high sedimentation values, there is a need for sediment management solutions. The proposed solution is the construction of a transverse breakwater north of the existing breakwater, spanning 300 meters. The design of the new breakwater is shown in **Figure 14.** with a black line.

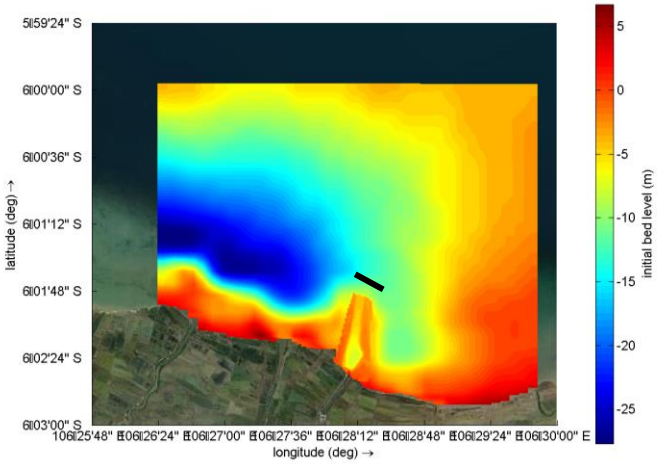

Figure 14. location of the new breakwater suggestion

The graph of sedimentation values or sediment addition of quarter time for the longitudinal section of the channel area after the implementation of the breakwater is shown in **Figure 15.**

Published by: Lembaga Penelitian dan Pengabdian Masyarakat (LPPM)
Institut Teknologi Sumatera, Lampung Selatan, Indonesia

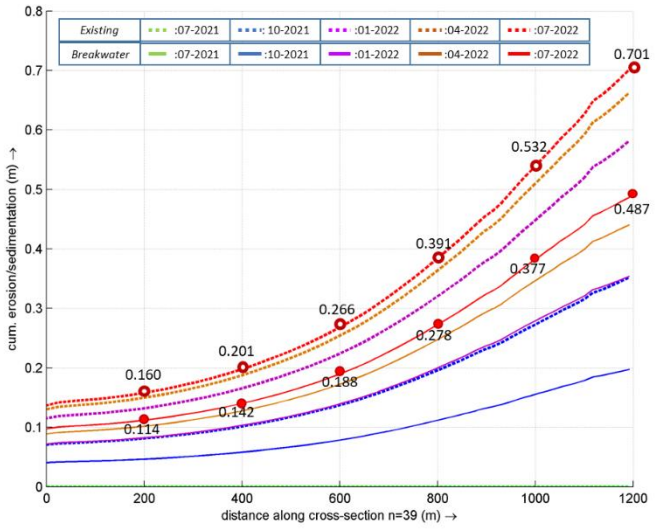

Figure 15. Graph of sediment addition values per quarterly after the installation of the new breakwater.

To observe the comparison of sedimentation value changes between the existing condition and after the installation of the new breakwater, refer to **Figure 16.**

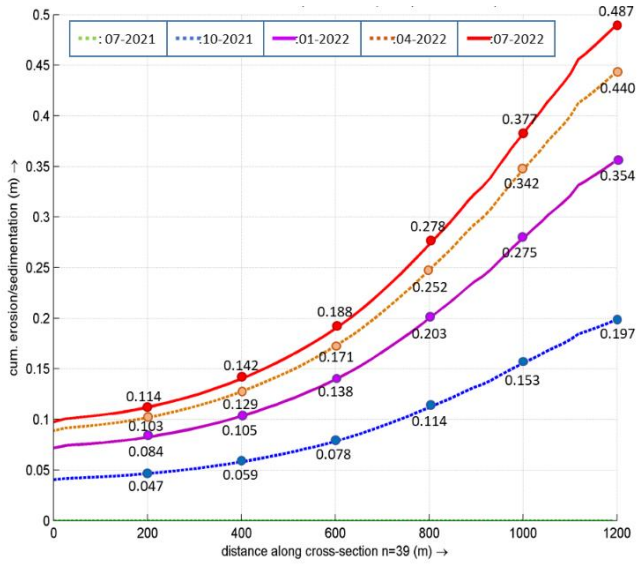

Figure 16. Graph of Sediment Addition Values per Quarterly: Existing Vs. Breakwater Addition.

From the graph, it can be observed that the addition of the new breakwater causes changes in sedimentation rates. For the intake area, the sedimentation rate decreases from 14 cm/year to 10 cm/year, resulting in an increase of 1.4 times in the service life of the intake area. In the first 200 meters of the turning basin area, the sedimentation rate changes from 16 cm/year to 11 cm/year, leading to a 1.4 times increase in the service life of the turning basin. In the navigation channel area, the sedimentation rate also undergoes changes. This leads to an average increase of 1.4 times in the service life of the navigation channel compared to the existing condition.

The installation of the new breakwater will extend the navigation channel beyond the existing breakwater. The sedimentation rate outside the existing breakwater changes, resulting in a 1.5 times increase in the dredging service life for the new navigation channel compared to the existing condition. The addition of the new breakwater reduces the sedimentation rate in the protected area (inside the canal) and increases the sedimentation rate on the north side of the breakwater.

Conclusion

The result of this study illustrates that the hydrodynamic condition in the Lontar steam-electric power plant can be effectively analyzed by using a combination of numerical modeling and qualitative assessment of in situ measurement data. The current conditions in the study area are influenced by tides from the sea and circulating water pump discharge. The tidal type is diurnal. Based on the model, it is found that sedimentation events occurring at the intake area and navigation channel, in general, are caused by the suction of the circulating water pump. The currents resulting from this suction lead to the transportation of sediment materials from areas outside the sediment control dam/breakwater, which then settle, particularly during high water level conditions due to the deceleration of flow velocity.

To minimize the sedimentation rate and extend the dredging service life, the author recommends installing a 300-meter-long breakwater with a longitudinal layout from the southeast to the northwest. The southeastern end of the breakwater should be positioned approximately 178 meters north of the eastern end of the existing breakwater/sediment control dam. This solution will extend the dredging service life in the intake area and navigation channel by 1.4-1.5 times. The initial dredging service life at the intake mouth of 10 years will increase to 14 to 15 years.

Acknowledgments

The authors gratefully acknowledge the support and contributions of the Ocean Engineering Program and Department of Oceanography, Institut Teknologi Sumatera, PLN Enjiniring, PT Suropati Hidro Energi and

PT Lapi Ganeshatama for the primary data, and Deltares for software and license.

References

[1] A. Kurniawan, A. Egon, K. A. Sujatmiko, and A. I. Malakani, "Hydrodynamic Modelling of Tidally-Influenced Fluvial Zone, a study case of Palembang, Indonesia," ILMU KELAUTAN: Indonesian Journal of Marine Sciences, vol. 27, no. 1, pp. 83–92, Mar. 2022, Accessed: Nov. 27, 2023. [Online]. Available: https://ejournal.undip.ac.id/index.php/ijms/article/view/41773/pdf

[2] C. Berenbrock and A. W. Tranmer, "Simulation of Flow, Sediment Transport, and Sediment Mobility of the Lower Coeur d'Alene River, Idaho," pubs.usgs.gov, 2008. https://pubs.usgs.gov/publication/sir20085093 (accessed Nov. 27, 2023).

[3] Deltares. User Manual Delft3D-FLOW, "Simulation of Multi-Dimensional Hydrodynamic Flows and Transport Phenomena, Including Sediments." Delft: Deltares ed, 2016.

[4] Egbert, G.D. & Erofeeva, S.Y "Efficient Inverse Modeling of Barotropic Ocean Tides", Journal of Atmospheric and Oceanic Technology, 2002 .

[5] G. R. Lesser, J. A. Roelvink, J. A. T. M. van Kester, and G. S. Stelling, "Development and validation of a three-dimensional morphological model," Coastal Engineering, vol. 51, no. 8–9, pp. 883–915, Oct. 2004, doi: https://doi.org/10.1016/j.coastaleng.2004.07.014.

[6] Li, M., Wang, Y.-p., Zhu, G., Yang, Y., Xiang, M., Lu, T., Cheng, J., Zhou, J., Zhang, J., Gao,J., "Suspended sediment transport in small and medium estuaries with the sluice gate: a case study of the Xinyanggang Estuary, China", Mar. Sci. Bull. 32,657–667, 2013.

[7] Li, M., Yang, Y., Xiang, M., Zhu, G., Lu, T., Zhou, J., Gao, J., Wang, Y.P. "Characteristics of suspended sediment and resuspension processes in Xinyanggang Estuary", J. Nanjing Univ. (Nat. Sci.) 5, 666–678, 2014.

[8] M. Álvarez, R. Carballo, V. Ramos, and G. Iglesias, "An integrated approach for the planning of dredging operations in estuaries," Ocean Engineering, vol. 140, pp. 73–83, Aug. 2017, doi: https://doi.org/10.1016/j.oceaneng.2017.05.014.

[9] I. M. Mason, "Algebraic reconstruction of a two-dimensional velocity inhomogeneity in the High Hazles seam of Thoresby colliery," Geophysics, vol. 46, no. 3, pp. 298–308, Mar. 1981, doi: https://doi.org/10.1190/1.1441200.

[10] P. Matte, Y. Secretan, and J. Morin, "Hydrodynamic Modeling of the St. Lawrence Fluvial Estuary. I: Model Setup, Calibration, and Validation," Journal of Waterway, Port, Coastal, and Ocean Engineering, vol. 143, no. 5, Sep. 2017, doi: https://doi.org/10.1061/(asce)ww.1943-5460.0000397.

[11] Q. Zhu et al., "Modeling morphological change in anthropogenically controlled estuaries," Anthropocene, vol. 17, pp. 70–83, Mar. 2017, doi: https://doi.org/10.1016/j.ancene.2017.03.001.

[12] S. D. Sandbach et al., "Hydrodynamic modelling of tidal-fluvial flows in a large river estuary," Estuarine, Coastal and Shelf Science, vol. 212, pp. 176–188, Nov. 2018, doi: https://doi.org/10.1016/j.ecss.2018.06.023.

[13] R. L. Soulsby and A. Wainwright, "A criterion for the effect of suspended sediment on near-bottom velocity profiles," Journal of Hydraulic Research, vol. 25, no. 3, pp. 341–356, May 1987, doi: https://doi.org/10.1080/00221688709499275.

[14] Van Maren, B, "An Introduction to Cohesive Sediment Transport Modelling" Delft: Deltares ed.2009.

[15] M. Zhang, I. Townend, H. Cai, and Y. Zhou, "Seasonal variation of tidal prism and energy in the Changjiang River estuary: a numerical study," Chinese Journal of Oceanology and Limnology, vol. 34, no. 1, pp. 219–230, Aug. 2015, doi: https://doi.org/10.1007/s00343-015-4302-8.

Published by: Lembaga Penelitian dan Pengabdian Masyarakat (LPPM)
Institut Teknologi Sumatera, Lampung Selatan, Indonesia